




Fitting the van Genuchten model to the measured hydraulic parameters in soils of different genesis and texture at the regional scale**

Bogusław Usowicz^{1,2}, Jerzy Lipiec¹*, Anna Siczek¹

¹Institute of Agrophysics, Polish Academy of Sciences, Doświadczalna 4, 20-290 Lublin, Poland

²Department of Civil Engineering and Environmental Sciences, Białystok University of Technology, Wiejska 45E, 15-351 Białystok, Poland

Received May 27, 2024; accepted July 18, 2024

Abstract. Soil hydraulic parameters are a key input for predicting soil water retention curves and water flow. The van Genuchten model is widely used to fit the van Genuchten hydraulic parameters including residual water content, saturated water content, a fitting parameter related to the inverse of the air entry pressure, and the shape parameter. This study aimed to show the interrelations of the soil hydraulic parameters on a large scale with both the inherent soil properties and the genetic type. The measured van Genuchten parameters originated from soil water retention curves determined in 100 pedons at 4 depths corresponding to the main soil diagnostic horizons. The results showed that the effect of soil texture on the van Genuchten hydraulic parameters was greater than that of the genetic soil type. The van Genuchten hydraulic parameters were in general significantly higher in fine-textured than coarse-textured soils. The vertical distribution of the hydraulic parameters was more discontinuous in fine- than in coarse-textured soils. The van Genuchten equation fits well to measured soil water retention ($R^2 > 0.885$) and thereby can predict the soil water retention curve for a variety of soils with acceptable uncertainty and improve soil water conservation on a large regional scale.

Keywords: soil hydraulic parameters, van Genuchten model, soil texture, genetic soil types, vertical distribution, regional scale

1. INTRODUCTION

The soil water retention curve (SWRC) relating water content (θ) and matric potential is a key property in quantifying the pore structure of soil (AL-Kayssi, 2021; Bondi *et al.*, 2022; Dexter and Czyż, 2007). It allows estimation of field water capacity, permanent wilting point, plant water availability (*e.g.* Fu *et al.*, 2021), water and heat flow processes (Heitman *et al.*, 2020; Usowicz and Lipiec, 2022), and soil compactness and quality (AL-Kayssi, 2021; Hessel *et al.*, 2022) and strength (Satyanaga *et al.*, 2022). The slope at the inflection of SWRC is used to assess the degradation of soil structure and soil physical quality (Dexter, 2004; Vizitiu *et al.*, 2011).

The SWRC and the saturated hydraulic conductivity are useful inputs for predicting hydraulic conductivity as a function of water matric potential $K(\psi)$. (Fuentes *et al.*, 2020; Lipiec *et al.*, 2021; Wang *et al.*, 2022).

The SWRC along with the $K(\psi)$ curve are important hydrodynamic characteristics used for the description of water and solute movement through the surface and subsurface in saturated and unsaturated porous soil (Khlosi *et*

*Corresponding author e-mail: j.lipiec@ipan.lublin.pl

**This work was partially funded by the HORIZON 2020, European Commission, Programme: H2020-SFS-2015-2: SoilCare for profitable and sustainable crop production in Europe, project No. 677407 (SoilCare, 2016-2021).

al., 2016; Szymkiewicz *et al.*, 2008; van Genuchten and Pachepsky, 2011). However, the measurement of SWRC is time-consuming and expensive, which restricts its application (van Looy *et al.*, 2017). Therefore, approaches for estimation (modelling) of SWRC based on inherent soil properties such as particle size distribution, organic matter content, plasticity index, and particle density using pedotransfer functions (PTFs) (Bai *et al.*, 2021; Rawls *et al.*, 2001; Wang *et al.*, 2021), neural network analyses (Minasny and McBratney, 2007), hyperspectral imaging (Krzyszczak *et al.*, 2023), and the hierarchical Bayesian probabilistic model (Yang *et al.*, 2015) are developed. The van Genuchten model (van Genuchten, 1980) is widely used to fit retention data (pairs of soil water content-soil water potential data) and extend measured values to the whole range of soil water content. The hydraulic parameters of the model equation include θ_s , θ_r , α , and n (AL-Kayssi, 2021; Du *et al.*, 2024; Usowicz *et al.*, 2011; Wösten *et al.*, 1999).

Using a sequence of empirical equations, Tian *et al.* (2018, 2020) extended the van Genuchten model to explain the effects of temporal variations in soil bulk density on changes in SWRCs. Other newly developed approaches allow estimating vG parameters and SWRC from soil electrical conductivity (Fu *et al.*, 2021), electrical resistivity (Lu *et al.*, 2020), and soil thermal conductivity along with texture, bulk density, and field capacity (Liu *et al.*, 2024). Recent results also indicate that the use of machine learning estimators has become an interesting tool to enhance the estimation of the soil water retention curve (SWRC) based on physical characterization parameters (Albuquerque *et al.*, 2022). The vG parameters are related to each other. In a study conducted by Fu *et al.* (2021) the relation allowed estimating the parameter α from the other vG parameters.

Although the approaches to estimate vG model parameters and, subsequently, the SWRC have been advanced for several decades, the effect of large-scale heterogeneity with consideration of both the genetic type and texture of soils in different environmental conditions has rarely been considered (Fu *et al.*, 2021). The heterogeneity in the soil texture can affect SWRC characteristics through the effect on pore size distribution, shape, and connectivity (Bondi *et al.*, 2022; Bouma and Anderson, 1997) and the impact of soil genetic types through the natural self-organization of soil as a result of specific soil-forming processes (Costantini and Mocali, 2022; Świtoniak *et al.*, 2022).

This study aimed to show the effect of varied soil characteristics on the van Genuchten model parameters and SWRCs in a range of soils. The RETC (retention curve computer code) program (van Genuchten *et al.*, 1991) was used to fit vG model parameters to measured soil water retention data from a previous survey comprising 100 pedons (Paluszczek, 2011; Usowicz, 2011). We hypothesized that the both soil genetic type and the soil texture affect the van Genuchten hydraulic parameters at the large regional scale. The pedons including the main horizons represented

the following genetic soil types: Luvisols derived from weathering silt formations, loess, loams, and loamy sands, Mollic Gleysols derived from loess-like deposits, loams, and loamy sands, and Phaeozems derived from loess. The soils derived from loess are prone to degradation by water and wind erosion, while those derived from sands are susceptible to agricultural drought. The degradation and recovery of the soils can be mediated by features of a given soil type associated with the pedogenesis process.

2. MATERIALS AND METHODS

The research was carried out in the central and south-eastern parts of Poland (traverse length of approximately 550 km) (Fig. 1). 100 soil pedons representing the following genetic types were analyzed: (A) Luvisols developed from silt formations; (B) Mollic Gleysols developed from silt formations; (C) Luvisols developed from loess; (D) Phaeozems developed from loess; (E) Luvisols developed from loams; (F) Mollic Gleysols developed from loams; (G) Luvisols developed from sands; (H) Mollic Gleysols developed from sands. The corresponding numbers of the pedons were: 16, 12, 12, 12, 12, 12, 8, and 16.

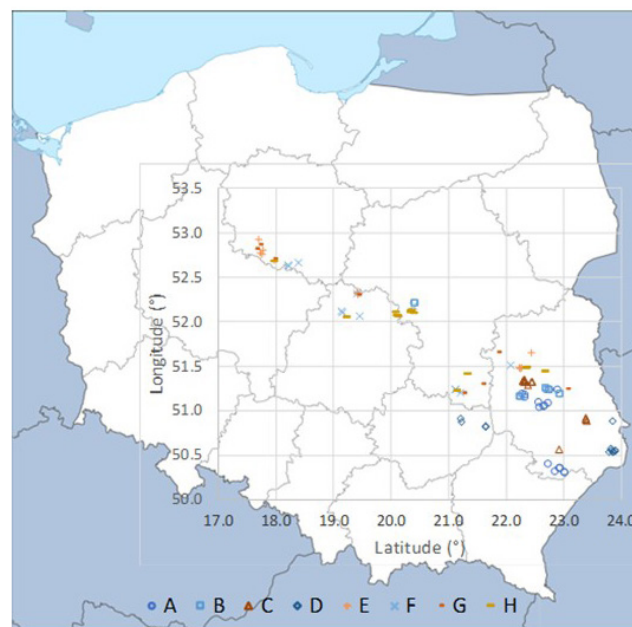


Fig. 1. Location of the studied soils: A – Luvisols developed from silt formations, B – Mollic Gleysols developed from silt formations, C – Luvisols developed from loess, D – Phaeozems developed from loess, E – Luvisols developed from loams, F – Mollic Gleysols developed from loams, G – Luvisols developed from sands, H – Mollic Gleysols developed from sands. The background map from https://pl.wikipedia.org/wiki/Plik:Poland_location_map_white.svg was modified using Microsoft Office PowerPoint 2019. Geographical coordinates of the studied soil pedons are in Table S1 (Supplementary material).

Bulk and undisturbed soil samples (in 4 replicates) were taken from the depths of 5-15, 30-40, 55-65, and 80-90 cm in all the soils. The depths correspond to the following diagnostic horizons: Eet, Bt, BC or C in Luvisols; Aa, Bbr, AC, Cg or G in Mollic Gleysols (depending on the subtype), and A, ABbr, Bbr or AC, Cca in Phaeozem soils (depending on the subtype) (Paluszek, 2011). A total 1 600 samples (100 pedons \times 4 depths/horizons \times 4 replicates) were used. All the soils were under cultivated cropland. The ploughing tillage system is usually used in the study area. The important threats limiting crop productivity are agricultural drought susceptibility and water erosion in central and south-eastern Poland, respectively.

The sampling was done immediately after harvest. The bulk samples were used to determine the particle size distribution using the sieving and hydrometer method (Ostrowska *et al.*, 1991) and soil organic carbon by dry combustion using the analyzer Vario Max CNS Elementar (Elementar, 2000). The data were collected within the project report "Criteria for assessing the physical condition of selected systematic units of arable soils" (Paluszek, 2011; Usowicz, 2011). Undisturbed soil in 100 cm³ steel cylinders (5.0 cm height) was used to determine the soil water retention curve (SWRC) with pressure plates (Soil Moisture Equipment Corp., Santa Barbara CA, USA) according to Richards' method (Klute and Dirksen, 1986a). After saturation, the following suction was consecutively applied to establish soil water matric potentials (in hPa): 1, 10, 31, 98, 155, 309, 490, 1554, 4900, and 15540 to obtain the SWRC. Saturated hydraulic conductivity was measured with the constant head method in soil samples of 100 cm³ using a laboratory permeameter (Eijkelkamp Agrisearch Equipments, The Netherlands) (Klute and Dirksen, 1986b).

The measured SWRCs were fit to the van Genuchten equation (van Genuchten, 1980) to derive the soil water retention curve and the hydraulic parameters with the RETC (retention curve computer code) (van Genuchten *et al.*, 1991). The van Genuchten equation is as follows:

$$\theta(h) = \theta_r + \frac{\theta_s - \theta_r}{[1 + (\alpha h)^n]^{1-1/n}},$$

where: θ_s – saturated water content (cm³ cm⁻³), θ_r – residual water content (cm³ cm⁻³), h – matric potential (–cm), α – fitting parameter related to the inverse of the air entry pressure (cm⁻¹), n – fitting parameter that determines the shape of the soil water retention curve (dimensionless).

The one-way analysis of variance (ANOVA) was performed for the θ_s , θ_r , $1/\alpha$, and n using STATISTICA 13.3 (StatSoft, Inc., Tulsa, OK, USA) to assess the effects of the genetic soil types (A-H) and the soil depths (5-15, 30-40, 55-65, and 80-90 cm). Mean comparisons were accomplished by the least significant difference (LSD) test at $p < 0.05$. The graphs were drawn by PRIMER Version 7 (Plymouth, UK).

3. RESULTS

3.1. Basic soil properties

The data in Table 1 show that the ranges of sand (2-0.05 mm), silt (0.05-0.002 mm), and clay (<0.002 mm) contents in the studied soils were 12.7-77.4%, 12.2-74.9%, and 4.6-20.0%, respectively. In general, lower contents of clay and higher contents of sand and silt were observed at the depth of 5-15 cm than at all the depths below. Based on the sand content, we divided the soils into two groups: (1) fine-textured soils, including Luvisols derived from silt formations, Mollic Gleysols derived from loess-like silt, and Luvisols and Phaeozems derived from loess (A-D) and (2) coarse-textured soils, including Luvisols derived from loams and sands and Mollic Gleysols derived from loams and sands (E-H). The sand contents in the first group and the second group of soils ranged from 12 to 40% and from 60 to 78%, respectively, at all depths. According to Hengl *et al.* (2017) and Huang and Hartemink (2020), the second group can be classified as sandy soils (sand content >50% and clay content <20%).

The bulk density (BD) of the soils varied from 1.36 to 1.74 Mg m⁻³ depending on the soil type and depth (Table 1). In general, the lowest BD values were recorded at the depth of 5-15 cm within the plough layer (1.36-1.55 Mg m⁻³) and increased in deeper soil correspondingly to the plough pan and/or the parent material (1.39-1.74 Mg m⁻³). Irrespective of the soil type, the densities were higher in the sandier soils associated in part with greater content of sand with high particle density.

The field water capacity (FWC) was higher in the fine-textured A-D soils (0.327-0.377 cm cm⁻³) than in the coarse-textured E-H soils (0.217-0.317 cm cm⁻³).

The saturated hydraulic conductivity (Ksat) varied from 22.5 to 248.5 cm day⁻¹ depending on the soil type and depth (Table 1). The Ksat values in most soils (B, C, F, G, H) were higher at the depth of 5-15 cm within the plough layer and appreciably lower at all three depths below. In the case of Phaeozems (D) and Luvisols derived from loams (E), the highest Ksat (72.8 and 114.5 cm day⁻¹) was noted at 55-65 or 80-90 cm, and the lowest values were recorded at 30-40 cm. The lowest Ksat at the depth of 30-40 cm within the plough pan of the D and E soils corresponded with the higher bulk densities (1.423 and 1.712 Mg m⁻³) than at the other depths in the pedon. The lowest differentiation of Ksat between the depths was recorded in Luvisols derived from silt formation (A): from 22.5 to 33.8 cm day⁻¹, and the largest range was noted in Luvisols derived from sands (G): from 108.6 to 401.4 cm day⁻¹.

The soil organic carbon content (SOC) ranged from 1.12 to 19.9 g kg⁻¹ depending on the soil type and depth (data not shown). The ranges of SOC (in g kg⁻¹) for the depths of 5-15, 30-40, 55-65, and 80-90 cm were 6.95-19.85, 2.08-12.69, 1.12-5.91, and 0.90-3.98, respectively. In all the soils, the SOC content decreased with depth. The highest organic carbon contents were recorded at the 5-15 cm

Table 1. Means and standard deviations of sand, silt and clay contents (%), bulk density (BD), field water capacity (FWC), and saturated hydraulic conductivity (Ksat) of the studied soils

Soils	Depth (cm)	Sand	Silt	Clay	BD	FWC	Ksat
		2-0.05 mm	0.05-0.002 mm	<0.002 mm	(Mg m ⁻³)	(cm ³ cm ⁻³)	(cm day ⁻¹)
A	5-15	20.69 (5.45)	70.88 (5.16)	8.44 (3.22)	1.419 (0.086)	0.359 (0.023)	27.0 (30.3)
	30-40	20.69 (6.7)	65.50 (8.5)	13.81 (5.56)	1.514 (0.078)	0.349 (0.027)	22.5 (30.3)
	55-65	32.94 (22.91)	47.88 (19.41)	19.19 (6.07)	1.583 (0.131)	0.324 (0.063)	33.8 (42.2)
	80-90	39.63 (24.91)	40.38 (21.56)	20.00 (6.28)	1.579 (0.179)	0.325 (0.083)	33.6 (47.9)
B	5-15	28.58 (7.51)	61.33 (6.41)	10.08 (3.37)	1.365 (0.116)	0.354 (0.023)	320.4 (288.7)
	30-40	26.25 (6.11)	61.67 (5.35)	12.08 (4.87)	1.389 (0.115)	0.353 (0.029)	226.1 (230.5)
	55-65	27.25 (7.92)	56.00 (9.01)	16.75 (7.29)	1.438 (0.106)	0.345 (0.025)	244.2 (309)
	80-90	37.00 (20.27)	46.33 (16.14)	16.67 (9.70)	1.501 (0.119)	0.327 (0.048)	94.0 (87.4)
C	5-15	15.08 (4.83)	72.58 (5.26)	12.33 (4.66)	1.394 (0.136)	0.336 (0.023)	79.9 (79.9)
	30-40	15.33 (4.81)	67.08 (6.1)	17.58 (4.58)	1.492 (0.068)	0.350 (0.023)	35.3 (38.6)
	55-65	16.00 (5.94)	65.17 (6.67)	18.83 (3.81)	1.475 (0.094)	0.347 (0.026)	56.7 (68.4)
	80-90	15.75 (5.19)	67.58 (7.19)	16.67 (3.60)	1.494 (0.121)	0.355 (0.041)	57.2 (81.3)
D	5-15	12.67 (1.56)	74.92 (2.39)	12.42 (2.75)	1.380 (0.087)	0.357 (0.023)	88.2 (101.9)
	30-40	12.92 (2.35)	71.50 (2.81)	15.58 (1.73)	1.423 (0.066)	0.362 (0.014)	26.0 (23.7)
	55-65	13.42 (2.23)	71.33 (2.02)	15.25 (1.22)	1.334 (0.111)	0.362 (0.021)	98.7 (57.8)
	80-90	13.33 (1.44)	72.00 (1.35)	14.67 (1.44)	1.399 (0.116)	0.377 (0.020)	72.8 (89.9)
E	5-15	62.25 (10.89)	28.92 (10.83)	8.83 (3.93)	1.547 (0.086)	0.275 (0.030)	89.9 (95.8)
	30-40	60.17 (6.77)	22.75 (6.74)	17.08 (6.33)	1.712 (0.118)	0.272 (0.024)	35.4 (38.7)
	55-65	59.67 (14.47)	21.75 (7.79)	18.58 (8.20)	1.708 (0.093)	0.263 (0.046)	54.1 (51.2)
	80-90	62.83 (14.57)	19.00 (8.56)	18.17 (7.96)	1.683 (0.111)	0.275 (0.031)	114.5 (164.2)
F	5-15	60.83 (7.38)	29.83 (9.13)	9.33 (3.60)	1.517 (0.227)	0.317 (0.060)	123.3 (125.8)
	30-40	61.08 (7.00)	26.25 (8.52)	12.67 (4.91)	1.601 (0.163)	0.290 (0.044)	56.8 (51.1)
	55-65	61.50 (12.50)	23.42 (11.5)	15.08 (6.36)	1.630 (0.082)	0.270 (0.040)	74.6 (62.7)
	80-90	64.42 (11.58)	18.58 (7.44)	17.00 (5.38)	1.635 (0.102)	0.264 (0.044)	91.1 (104.2)
G	5-15	72.63 (2.88)	22.63 (3.85)	4.75 (3.24)	1.546 (0.104)	0.259 (0.035)	401.4 (809.5)
	30-40	77.38 (10.62)	16.00 (7.78)	6.63 (4.63)	1.673 (0.083)	0.217 (0.049)	248.5 (359.2)
	55-65	67.25 (12.60)	16.50 (8.19)	16.25 (7.30)	1.707 (0.041)	0.254 (0.038)	150.3 (214.8)
	80-90	72.00 (11.38)	12.25 (5.80)	15.75 (6.36)	1.739 (0.077)	0.251 (0.042)	108.6 (185.6)
H	5-15	73.69 (7.72)	21.69 (7.54)	4.63 (3.16)	1.503 (0.116)	0.286 (0.037)	233.1 (289.2)
	30-40	76.50 (7.25)	17.25 (6.18)	6.25 (4.92)	1.639 (0.097)	0.237 (0.049)	130.9 (188.1)
	55-65	73.38 (10.29)	15.38 (5.83)	11.25 (7.78)	1.655 (0.127)	0.225 (0.060)	147.8 (186.0)
	80-90	71.19 (9.74)	15.81 (4.25)	13.00 (6.91)	1.688 (0.095)	0.251 (0.042)	75.0 (77.8)

A – Luvisols developed from silt formations, B – Mollic Gleysols developed from silt formations, C – Luvisols developed from loess, D – Phaeozems developed from loess, E – Luvisols developed from loams, F – Mollic Gleysols developed from loams, G – Luvisols developed from sands, H – Mollic Gleysols developed from sands.

depth of Mollic Gleysols and Phaeozems (from 11.6 to 19.9 g kg⁻¹), and the lowest levels were noted in Luvisols (0.9-1.2 g kg⁻¹) at the 80-90 cm depth. The vertical distribution was less variable in Mollic Gleysols and Phaeozems than in Luvisols. The depth-averaged means (5-90 cm) of the soil organic carbon content varied from 2.90-3.35 g kg⁻¹ in Luvisols (A, C, E, G) to 6.26-9.8 g kg⁻¹ in Mollic Gleysols and Phaeozems (B, D, F, H).

3.2. Van Genuchten parameters

3.2.1. Fine-textured soils (A-D)

3.2.1.1. Luvisols developed from silt formations (A)

Table 2 demonstrates that the residual water content (θ_r) varied from 0.0327 cm³ cm⁻³ at the 30-40 cm depth to 0.0611 cm³ cm⁻³ at 80-90 cm. The values of θ_s , negative pressure heads at which air starts entering the soil matrix ($1/\alpha$) (α = scaling parameter), and shape parameters (n) in the soil pedon had a parabolic shape with the lowest values at 55-65 cm (0.388 cm³ cm⁻³, 155.2 cm, and 1.396, respectively), and the highest values were obtained at 5-15 cm (0.417 cm³ cm⁻³, 301.1 cm, and 1.733, respectively). This similar distribution implies an existing positive relationship between the three vG parameters. The differences in all the vG parameters values between the depths were in most cases not significant ($p < 0.05$) except the higher values of $1/\alpha$ and n at 5-15 cm vs. 55-65 cm.

3.2.1.2. Mollic Gleysols developed from loess-like silt formations (B)

As can be seen from Table 2, θ_r increased from 0.0027 cm³ cm⁻³ at 5-15 cm to 0.0115-0.0172 cm³ cm⁻³ at all the deeper layers, while θ_s decreased from 0.439 at the top 5-15 cm to 0.407 cm³ cm⁻³ at 80-90 cm. Both $1/\alpha$ and n had the lowest value at the 5-15 cm depth (87.13 cm and 1.255, respectively) and increased in the deeper soil to 175 cm and 1.493 at the 80-90 cm depth. The differences in all the vG parameters values between the depths were not significant ($p < 0.05$).

3.2.1.3. Luvisols developed from loess (C)

The θ_r had the lowest value at the top three upper layers (0.0211-0.0301 cm³ cm⁻³) and increased to 0.0513 cm³ cm⁻³ at the 80-90 cm depth (Table 2). θ_s was similar in all four depths (0.399 to 0.421 cm³ cm⁻³). The course of $1/\alpha$ and n in the soil profile was similar, with the highest values at the 80-90 cm depth (372.52 cm and 1.840, respectively) and the lowest values at 55-65 cm (208.79 cm and 1.412, respectively). The θ_r , $1/\alpha$, and n values were significantly ($p < 0.05$) lower at 55-65 vs. 80-90 cm.

3.2.1.4. Phaeozems developed from loess (D)

The lowest θ_r value (0.0123 cm³ cm⁻³) was recorded at 55-65 cm, and the highest value of this parameter (0.0419 cm³ cm⁻³) was noted at 80-90 cm (Table 2). The θ_s values were similar at all the depths and varied from 0.417 to 0.451. $1/\alpha$

Table 2. Means (n=4) of the van Genuchten parameters including residual water content (θ_r), saturated water content (θ_s), matric water potentials at which air starts entering the soil ($1/\alpha$ where α is a fitting parameter related to the inverse of the air entry potential, fitting parameter that determine the shape of the soil water retention curve (n)). Different letters indicate a significant difference between depths within the same soil by the LSD test ($p < 0.05$)

Soil	Depth (cm)	θ_r	θ_s	$1/\alpha$	n
		(cm ³ cm ⁻³)		(cm)	
A	5-15	0.0433 a	0.417 a	301.1 b	1.733 b
	30-40	0.0327 a	0.400 a	240.4 ab	1.538 ab
	55-65	0.0469 a	0.388 a	155.2 a	1.396 a
	80-90	0.0611 a	0.393 a	189.9 ab	1.500 ab
B	5-15	0.0027 a	0.439 a	87.1 a	1.255 a
	30-40	0.0172 a	0.429 a	137.9 a	1.328 a
	55-65	0.0115 a	0.423 a	150.6 a	1.374 a
	80-90	0.0126 a	0.407 a	175.6 a	1.493 a
C	5-15	0.0211 a	0.421 a	232.1 ab	1.501 ab
	30-40	0.0301 ab	0.401 a	287.2 ab	1.566 ab
	55-65	0.0211 a	0.408 a	208.7 a	1.412 a
	80-90	0.0513 b	0.399 a	372.5 b	1.84 b
D	5-15	0.0207 ab	0.432 ab	225.8 ab	1.454 ab
	30-40	0.0316 ab	0.417 a	257.6 ab	1.509 ab
	55-65	0.0123 a	0.451 b	168.0 a	1.448 a
	80-90	0.0419 b	0.430 ab	317.9 b	1.732 b
E	5-15	0.0116 a	0.390 b	79.0 a	1.306 b
	30-40	0.0064 a	0.337 a	50.5 a	1.184 a
	55-65	0.0198 a	0.348 a	76.2 a	1.24 ab
	80-90	0.0031 a	0.356 ab	78.2 a	1.224 ab
F	5-15	0.0383 b	0.384 a	166.6 b	1.375 b
	30-40	0.0116 a	0.375 a	51.5 a	1.195 a
	55-65	0.0059 a	0.375 a	64.6 ab	1.246 ab
	80-90	0.0006 a	0.380 a	45.2 a	1.181 a
G	5-15	0.0056 a	0.389 b	81.9 a	1.379 a
	30-40	0.0004 a	0.361 ab	62.6 a	1.323 a
	55-65	0.0100 a	0.347 a	53.4 a	1.249 a
	80-90	0.0170 a	0.334 a	80.6 a	1.252 a
H	5-15	0.0147 a	0.405 b	81.5 a	1.369 a
	30-40	0.0078 a	0.361 a	30.9 a	1.287 a
	55-65	0.0091 a	0.367 a	39.1 a	1.317 a
	80-90	0.0135 a	0.353 a	78.3 a	1.337 a

Explanations as in Table 1.

and n were similarly distributed in the soil profile, with the lowest values at 55-65 cm (168.0 cm and 1.444, respectively) and the highest levels at 80-90 cm (317.94 cm and 1.732, respectively) (Table 2). The θ_r , $1/\alpha$, and n values were higher ($p < 0.05$) at 55-65 vs. 80-90 cm, and θ_s had a higher value at 30-40 vs. 55-65 cm.

3.2.2. Coarse-textured soils

3.2.2.1. Luvisols developed from loams (E)

The lowest θ_r values were recorded at 30-40 and 80-90 cm (0.0031-0.0064 $\text{cm}^3 \text{cm}^{-3}$), whereas those noted at 5-15 and 55-65 cm were appreciably higher (0.0116-0.0198 $\text{cm}^3 \text{cm}^{-3}$) (Table 2). θ_s was higher at 5-15 cm (0.390 $\text{cm}^3 \text{cm}^{-3}$) than at the other depths (0.337-0.356 $\text{cm}^3 \text{cm}^{-3}$). The $1/\alpha$ and n parameters had the lowest values at 30-40 cm (50.57 cm and 1.184, respectively) and increased at the other depths (76.24-79.04 cm and 1.224-1.306, respectively). The θ_r and n values were higher ($p < 0.05$) at the top 5-15 cm vs. all the depths below.

3.2.2.2. Mollic Gleysols developed from loams (F)

The value of θ_r was appreciably higher at 5-15 cm (0.0383 $\text{cm}^3 \text{cm}^{-3}$) than at all the depths below (0.0006-0.0116 $\text{cm}^3 \text{cm}^{-3}$) (Table 2). θ_s was similar at all the depths (0.375-0.384 $\text{cm}^3 \text{cm}^{-3}$). $1/\alpha$ and n had a similar vertical distribution with higher values at 5-15 cm (166.69 cm and 1.375, respectively) than at all the depths below (45.24-64.67 cm and 1.181-1.246, respectively). The maxima of

the θ_r , $1/\alpha$, and n values at 5-15 cm were significantly higher vs. those at all the other depths ($p < 0.05$) with θ_r and vs. 30-40 and 80-90 cm with $1/\alpha$ and n .

3.2.2.3. Luvisols developed from sands (G)

The θ_r values varied from 0.0004 at the 30-40 cm depth to 0.0170 $\text{cm}^3 \text{cm}^{-3}$ at 80-90 cm (Table 2). The highest θ_s at 5-15 cm (0.389 $\text{cm}^3 \text{cm}^{-3}$) decreased with depth to 0.334 $\text{cm}^3 \text{cm}^{-3}$ at 80-90 cm. $1/\alpha$ and n had a similar vertical distribution with minimum values at 55-65 cm (53.48 cm and 1.249, respectively) and maximum values at 5-15 cm (81.98 cm and 1.379, respectively). The maximum θ_s at 5-15 cm was significantly ($p < 0.05$) higher vs. the two depths within 55-90 cm.

3.2.2.4. Mollic Gleysols developed from sands (H)

The θ_r values were in general low in the soil profile (from 0.0078 to 0.0147 $\text{cm}^3 \text{cm}^{-3}$) (Table 2). The values of θ_s at 5-15 cm were higher vs. all the other depths ($p < 0.05$). $1/\alpha$ and n had a similar vertical distribution with maxima at the depth of 0-15 cm (81.55 cm and 1.369, respectively) and minimum (30.9 cm, 1.287) at the depth of 30-40 cm.

3.3. Interrelations of van Genuchten parameters, soil type, and soil texture

The data presented in Fig. 2 show that the depth-averaged means of θ_r varied from 0.0266 to 0.046 $\text{cm}^3 \text{cm}^{-3}$ in 3 of the 4 fine-textured soils, including Luvisols derived from silt formations and from loess (A, C) and Phaeozems from loess (D); they were significantly higher ($p < 0.05$) than the values ranging from 0.0083 to 0.0113 $\text{cm}^3 \text{cm}^{-3}$ in all the coarse-textured soils, including Luvisols derived from loams and sands (E, G) and Mollic Gleysols derived

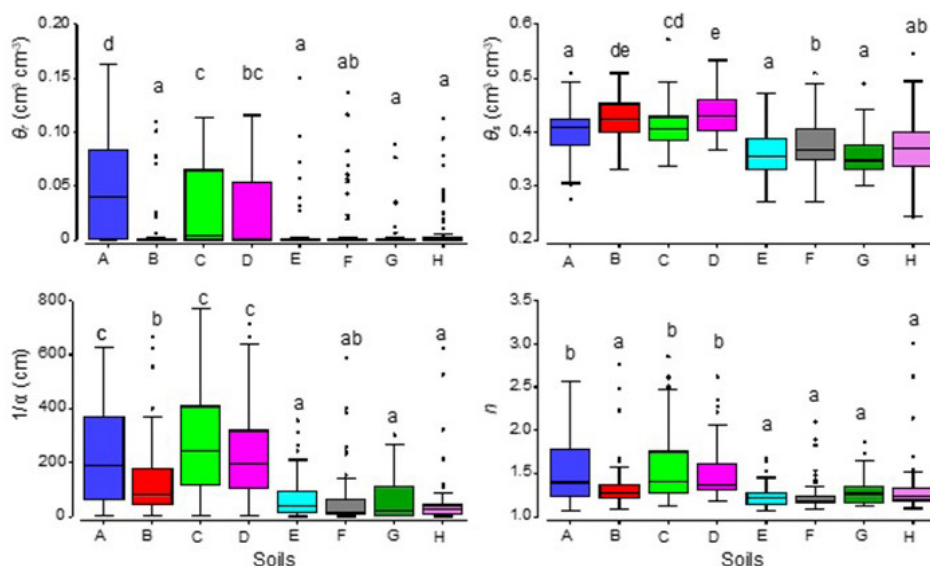


Fig. 2. Mean comparisons of the main effect of soils on residual water content (θ_r), saturated water content (θ_s), matric water potentials at which air starts entering the soil ($1/\alpha$ where α is a fitting parameter related to the inverse of the air entry potential), and fitting parameter that determines the shape of the soil water retention curve (n). Horizontal lines, vertical bars, and dots indicate the median, and range of non-outliers and outliers. Different letters indicate statistically significant differences ($p < 0.05$).

from sands (H). In the case of the fine-textured Mollic Gleysols from loess-like silt, the θ_r value was not different ($p < 0.05$) from that in each soil within the coarse-textured group (E-H).

Also, θ_s in the soils were higher in the fine-textured group (0.3996 to 0.4325 $\text{cm}^3 \text{cm}^{-3}$) than in the coarse-textured soils (0.3577-0.3785 $\text{cm}^3 \text{cm}^{-3}$). In most cases, the θ_s values of the fine- vs. coarse-textured soils were statistically significantly different ($p < 0.05$).

The mean soil water matric potentials at which air starts entering the soil matrix ($1/\alpha$) varied within the fine-textured soils from 137.9 cm in Mollic Gleysols (B) to 275.2 cm in Luvisols (C) and within the coarse-textured soils from 57.5 cm in Mollic Gleysols derived from sands (H) to 82 cm in Mollic Gleysols derived from loams (F). In most cases (except B and F Mollic Gleysols), the differences in the $1/\alpha$ values between each fine-textured soil vs. each coarse-textured soil were significant ($p < 0.05$), irrespective of the genetic soil type.

The mean values of the shape parameter (n) varied in the fine-textured soils from 1.3626 in Mollic Gleysols (B) to 1.5799 in Luvisol (C) and within the coarse-textured soils from 1.2387 in Luvisols (E) to 1.3276 Mollic Gleysols (H) (Fig. 2). The differences in n between each fine-textured soil vs. each coarse-textured soil were significant ($p < 0.05$) except for the fine-textured B soil and all the coarse-textured soils. The higher mean values of the shape parameter (n) in the fine-textured (A-D) soils (1.3626-1.5799) than in the coarse-textured (E-H) soils (1.25-1.32) indicate greater steepness of SWRCs in the latter.

Figure 3 shows that the soil type-averaged means of θ_r varied insignificantly from 0.0181 at 30-40 cm to 0.0264 at 80-90 cm. The θ_s values were higher ($p < 0.05$) at the 5-15 cm

depth than at the other depths. Both $1/\alpha$ and n values were higher ($p < 0.05$) at 5-15 than at 55-65 cm. The analysis of the mean values and standard deviations indicates that the distribution of the van Genuchten parameters in soil pedon depths was in general more discontinuous in the fine-textured than coarse-textured soils.

The high coefficients of determination R^2 (0.885-1.00) (Table S1) showed that the van Genuchten soil water retention model yields acceptable results for the large set of data measured for different genetic soil types, textures, and pedon depths on a large scale.

4. DISCUSSION

Our results showed that the residual water content (θ_r) retained in small pores was, in general, higher (0.0266-0.046 $\text{cm}^3 \text{cm}^{-3}$) in the fine-textured soils (A, C, D) derived from silt formations and loess (except the lower value in soil B derived from loess-like deposits) than in the coarse-textured soils (E-H) derived from sands and loams (0.0083 to 0.0113 $\text{cm}^3 \text{cm}^{-3}$), irrespective of the genetic soil type (Fig. 2). The higher θ_r values in the fine- than coarse-textured soils reflect a positive association between particle size and pore size and the related stronger adsorption capacity (e.g. Kumar *et al.*, 2019). Noteworthy is the relatively low θ_r in Mollic Gleysols (B) derived from loess-like deposits compared to Phaeozems and Luvisols and Mollic Gleysols derived from loess. This difference can be related to the greater content of the sand fraction (2-0.05 mm) in soils derived from loess-like deposits (B) than from loess (C, D) (Table 1). The greater amount of the sand fraction in loess-like deposits (B) is attributed to their origin from the weathering of Holocene dust and fluvioglacial and limnoglacial

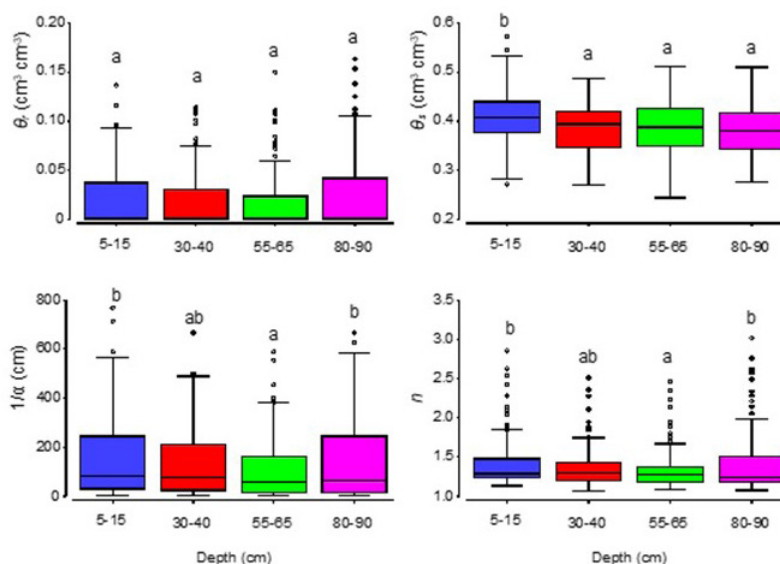


Fig. 3. Mean comparisons of the main effect of depths on residual water content (θ_r), saturated water content (θ_s), and matric water potentials at which air starts entering the soil ($1/\alpha$ where α is a fitting parameter related to the inverse of the air entry potential), and fitting parameter that determines the shape of the soil water retention curve (n). Horizontal lines, vertical bars, and dots indicate the median, and range of non-outliers and outliers, respectively. Different letters indicate statistically significant differences ($p < 0.05$).

sediments in contrast to loess deposited by wind (Maruszczak, 2000). Also, the saturated water content (θ_s) was greater in the fine-textured (0.3996–0.4325 cm³ cm⁻³) vs. coarse-textured soils (0.3577–0.3785 cm³ cm⁻³), which can be attributed to better aggregation (*e.g.* Bieganowski *et al.*, 2018) and greater contribution of large inter-aggregate pores (structural porosity) (Lipiec *et al.*, 2007).

The matric water potentials at which air starts entering the soil matrix ($1/\alpha$) were significantly higher (137.9–275.2 cm) in the fine-textured (A–D) than in coarse-textured (E–H) soils (from 57.5 to 82 cm). The higher values of the air entry matric potential promote infiltration and storage of water during rainfall periods and impede drainage and loss of water during prolonged drying periods, thereby increasing resistance to extreme weather conditions associated with progressive climate changes (Bondi *et al.*, 2022). The resistance can be further enhanced by the higher field water capacity (FWC) in the fine-textured (0.327–0.377 cm³ cm⁻³) vs. coarse-textured (0.217–0.317 cm³ cm⁻³) soils (Table 1). Irrespective of the texture, the Mollic Gleysols (B, F, H) and Phaeozems (D) compared to the other soil types can be more resilient to increased drought incidence due to the higher average content of SOC in the whole soil pedon (6.26–9.8 vs. 2.90–3.35 g kg⁻¹) through increasing water storage (Lipiec *et al.*, 2021). The lower $1/\alpha$ values of the coarse-textured soils signify larger sizes of macropores (Fu *et al.*, 2021), which result in better drainage and aeration following soil saturation with water, as they empty first as the matric potential decreases (Jabro and Stevens, 2022). Further ongoing studies aiming at the estimation of hydraulic conductivity as a function of the water matric potential based on the water retention and saturated hydraulic conductivity data collected using the van Genuchten equation will improve the evaluation of the resistance to climate change in terms of movement and accessibility of water for plant roots in various site conditions.

Overall, our study demonstrated that the differences in the values of all the vG parameters were appreciably high between the soils from the different textural groups, irrespective of the genetic soil type, and much lower and in general statistically insignificant ($p < 0.05$) between the genetic soil types within the same textural groups. For example, within the coarse-textured soils, all the vG parameters were not different between two Luvisols (E and G) and between two Mollic Gleysols (F and H). This observation indicates the suitability of soil texture data for the prediction of vG parameters in large scales that require a description of hydraulic properties at smaller core and/or pore scales (Hopmans *et al.*, 2002; Vogel, 2019). The suitability can be enhanced by the worldwide availability of quantitative data on textural fractions in soil geographic databases (*e.g.* Batjes *et al.*, 2020; Hengl *et al.*, 2017) or the Soil Quality Mobile App (SQAPP) (Fleskens *et al.*, 2020).

Using the same sampling and measurement procedure with pressure plates in this study was suitable for the reliable comparison of soil water retention between different soils at the regional scale. However, recent studies revealed substantial differences in the measurement of soil water retention curves due to variability in measurement procedures used in different laboratories (Mosquera *et al.*, 2021; Guillaume *et al.*, 2023). The variability results mostly from the different devices used, sample size, saturation procedure, inadequate hydraulic contact in suction plate or pressure plate methods, or weighting technique (Guillaume *et al.*, 2023). The mean inter-laboratory variability in the wet part of the SWRCs was more essential than the variability due to intrinsic differences between soil samples. Another source of variability of soil water retention outcomes from measurements at field and laboratory scales. In a study by Pachepsky *et al.* (2001) field vs. laboratory measurement of water retention in fine-textured soils was significantly smaller due to different soil volumes and spatial scales. To improve both comparison of differently determined SWRC and hydraulic databases further studies are required for standardization and harmonization of methods (Guillaume *et al.*, 2023).

5. CONCLUSIONS

The results of this study showed the following findings:

1. The van Genuchten type function fitted very well to the measured soil water retention parameters, including residual water content, saturated water content, matric water potentials at which air starts entering the soil, and the shape parameter ($R^2 > 0.885$) for a range of soils with different texture and genesis in central and south-eastern Poland. This indicates good performance of the van Genuchten model at a large regional scale.
2. The van Genuchten parameters were higher in the fine-textured compared to coarse-textured soils. They were less influenced by the genetic type than the soil texture.
3. The vertical distribution of the van Genuchten parameters was in general more discontinuous in the fine-textured than coarse-textured soils.
4. The results support our hypothesis that the soil texture and genetic type have a different effect on the van Genuchten hydraulic parameters across the pedon and regional scale.

Conflicts of Interest: The authors declare no competing interests.

Data availability: Data will be made available on request from the corresponding author – Jerzy Lipiec.

Author contributions: B.U. – conceptualization, investigation, formal analysis; J.L. – conceptualization, writing – original draft; A.S. – formal analysis, visualization. All authors reviewed the manuscript.

6. REFERENCES

- Albuquerque, E.A.C., de Faria Borges, L.P., Cavalcante, A.L.B., Machado, S.L., 2022. Prediction of soil water retention curve based on physical characterization parameters using machine learning. *Soils Rocks*, São Paulo 45(3):e2022000222. <https://doi.org/10.28927/SR.2022.000222>
- AL-Kayssi, A.W., 2021. Use of water retention data and soil physical quality index S to quantify hard-setting and degree of soil compactness indices of gypsiferous soils. *Soil Till. Res.* 206, 104805. <https://doi.org/10.1016/j.still.2020.104805>
- Bai, X., Shao, M.A., Jia, X.X., Zhao, C.L., 2022. Prediction of the van Genuchten model soil hydraulic parameters for the 5-m soil profile in China's Loess Plateau. *Catena* 210, 105889. <https://doi.org/10.1016/j.catena.2021.105889>
- Batjes, N.H., Ribeiro, E., van Oostrum, A., 2020. Standardised soil profile data to support global mapping and modelling (WoSIS snapshot 2019). *Earth System Science Data* 12, 299-320. <https://doi.org/10.5194/essd-12-299-2020>
- Bieganowski, A., Zaleski, T., Kajdas, B., Sochan, A., Józefowska, A., Beczek, M., *et al.*, 2018. An improved method for determination of aggregate stability using laser diffraction. *Land Degradation Develop.* 29(5), 1376-1384. [doi:10.1002/ldr.2941](https://doi.org/10.1002/ldr.2941)
- Bondi, C., Castellini, M., Iovino, M., 2022. Compost amendment impact on soil physical quality estimated from hysteretic water retention curve. *Water* 14, 1002. <https://doi.org/10.3390/w14071002>
- Bouma, J., Anderson, J.L., 1997. Water movement through pedal soils. I. Saturated flow. *Soil Sci. Soc. Am. J.* 41, 413-418.
- Costantini, E.A.C., Mocali, S., 2022. Soil health, soil genetic horizons and biodiversity. *J. Plant Nutr. Soil Sci.* 185, 24-34. [doi:10.1002/jpln.202100437](https://doi.org/10.1002/jpln.202100437)
- Dexter, A.R., 2004. Soil physical quality: part III. Unsaturated hydraulic conductivity and general conclusions about S theory. *Geoderma* 120: 227-239. [doi:10.1016/j.geoderma.2003.09.006](https://doi.org/10.1016/j.geoderma.2003.09.006)
- Dexter, A.R., Czyż, E.A., 2007. Applications of S-theory in the study of soil physical degradation and its consequences. *Land Degradation Develop.* 18, 369-381. <https://doi.org/10.1002/ldr.779>
- Du, C., Lu, X., Yi, F., 2024. Impact of modifiers on soil-water characteristics of graphite tailings. *Sci. Rep.* 14, 4186. <https://doi.org/10.1038/s41598-024-52826-6>
- Flekens, L., Ritsema, C., Bai, Z., Geissen, V., Mendes de Jesus, J., da Silva, V., *et al.*, 2020. Tested and validated final version of SQAPP (143 pp.) iSQAPER Project Deliverable 4.2. The Soil Quality Mobile App (SQAPP). www.isqaper-is.eu.
- Fu, Y., Horton, R., Heitman, J., 2021. Estimation of soil water retention curves from soil bulk electrical conductivity and water content measurements. *Soil Till. Res.* 209, 104948. [doi:10.1016/j.still.2021.104948](https://doi.org/10.1016/j.still.2021.104948)
- Fuentes, C., Chávez, C., Brambila, F., 2020. Relating hydraulic conductivity curve to soil-water retention curve using a fractal model. *Mathematics* 8, 2201. [doi:10.3390/math8122201](https://doi.org/10.3390/math8122201)
- Guillaume, B., Aroui Boukbida, H., Bakker, G., Bieganowski, A., Brostaux, Y., Cornelis, W., *et al.*, 2023. Reproducibility of the wet part of the soil water retention curve: A European interlaboratory comparison. *EGUsphere* 9, 1-23. <https://doi.org/10.5194/egusphere-2022-1496>
- Heitman, J., Zhan, X., Xiao, X., Ren, T., Horton, R., 2020. Advances in heat-pulse methods: Measuring soil water evaporation with sensible heat balance. *Soil Sci. Soc. Am. J.* 84, 1371-1375. <https://doi.org/10.1002/saj2.20149>
- Hengl, T., Mendes de Jesus, J., Heuvelink, G.B.M., Ruiperez Gonzalez, M., Kilibarda, M., Blagotić, A., *et al.*, 2017. SoilGrids250m: Global gridded soil information based on machine learning. *PLoS ONE* 12 (2), e0169748. <https://doi.org/10.1371/journal.pone.0169748>
- Hessel, R., Wyseure, G., Panagea, I.S., Alaoui, A., Reed, M.S., van Delden, H., *et al.*, 2022. Soil-improving cropping systems for sustainable and profitable farming in Europe. *Land* 11, 780. <https://doi.org/10.3390/land11060780>
- Hopmans, J.W., Nielsen, D.R., Bristow, K.L., 2002. How useful are small-scale soil hydraulic property measurements for large-scale vadose zone modeling. In: D. Smiles, P.A.C. Raats, A. Warrick (Eds.), *Heat and Mass Transfer in the Natural Environment*, The Philip Volume AGU, Geophysical Monograph Series No. 129, 247-258.
- Huang, J., Hartemink, A.E., 2020. Soil and environmental issues in sandy soils. *Earth-Science Reviews* 208, 103295. <https://doi.org/10.1016/j.earscirev.2020.103295>
- Jabro, J.D., Stevens, W.B., 2022. Pore size distribution derived from soil-water retention characteristic curve as affected by tillage intensity. *Water* 14, 3517. <https://doi.org/10.3390/w14213517>
- Khlosi, M., Alhamdoosh, M., Douaik, A., Gabriels, D., Cornelis, W.M., 2016. Enhanced pedotransfer functions with support vector machines to predict water retention of calcareous soil. *Eur. J. Soil Sci.* 67, 276-284.
- Klute, A., Dirksen, C., 1986a. Water retention. Laboratory methods. In: A. Klute (Ed.), *Methods of Soil Analysis. Part I. Physical and Mineralogical Methods*. SSA Book Series Vol. 5.
- Klute, A., Dirksen, C. 1986b. Hydraulic conductivity and diffusivity: Laboratory methods. In: A. Klute (Ed.), *Methods of Soil Analysis. Part I. Physical and Mineralogical Methods*. SSA Book Series Vol. 5.
- Krzyszczak, J., Baranowski, P., Pastuszka-Woźniak, J., Wesółowska, M., Cymerman, J., Sławiński, C., *et al.*, 2023. Assessment of soil water retention characteristics based on VNIR/SWIR hyperspectral imaging of soil surface. *Soil Till. Res.* 233, 105789. [doi:10.1016/j.still.2023.105789](https://doi.org/10.1016/j.still.2023.105789)
- Kumar, P.S., Korving, L., Keesman, K.J., van Loosdrecht, M.C.M., Witkamp, G.J., 2019. Effect of pore size distribution and particle size of porous metal oxides on phosphate adsorption capacity and kinetics. *Chemical Eng. J.* 358, 160-169. <https://doi.org/10.1016/j.cej.2018.09.202>
- Lipiec, J., Usowicz, B., Kłopotek, J., Turski, M., Frąć, M., 2021. Effects of application of recycled chicken manure and spent mushroom substrate on organic matter, acidity, and hydraulic properties of sandy soils. *Materials* 14, 4036. <https://doi.org/10.3390/ma14144036>
- Lipiec, J., Walczak, R., Witkowska-Walczak, B., Nosalewicz, A., Słowińska-Jurkiewicz, A., Sławiński, C., 2007. The effect of aggregate size on water retention and pore structure of silt loam soils of different genesis. *Soil Till. Res.* 97, 239-246. <https://doi.org/10.1016/j.still.2007.10.001>
- Liu, L., Lu, Y., Horton, R., Ren, T., 2024. Determination of soil water retention curves from thermal conductivity curves, texture, bulk density, and field capacity. *Soil Till. Res.* 237, 105957. <https://doi.org/10.1016/j.still.2023.105957>

- Lu, D., Wang, H., Huang, D., Li, D., Sun, Y., 2020. Measurement and estimation of water retention curves using electrical resistivity data in porous media. *J. Hydrologic Eng.* 25(6). [http://dx.doi.org/10.1061/\(ASCE\)HE.1943-5584.0001925](http://dx.doi.org/10.1061/(ASCE)HE.1943-5584.0001925)
- Maruszczak, H., 2000. Definition and classification of loesses and loess-like deposits (in Polish). *Przegląd Geologiczny* 48, 580-586.
- Minasny, B., McBratney, A. B., 2007. Estimating the water retention shape parameter from sand and clay content, *Soil Sci. Soc. Am. J.* 71, 1105-1110.
- Mosquera, G. M., Franklin, M., Jan, F., Rolando, C., Lutz, B., David, W., *et al.*, 2021. A field, laboratory, and literature review evaluation of the water retention curve of volcanic ash soils: How well do standard laboratory methods reflect field conditions?, *Hydrol. Proc.* 35, e14011, <https://doi.org/10.1002/HYP.14011>
- Ostrowska, A., Gawliński, S., Szczubiałka, Z., 1991. Analyses and Evaluation Methods of Soil and Plants (in Polish). Institute of Environmental Protection, Warsaw, pp. 334.
- Paluszek, J., 2011. Criteria of evaluation of soil physical quality of polish arable soils (in Polish). *Acta Agrophysica* 191, 1-139.
- Pachepsky, Y.A., Rawls, W.J., Gimenez, D., 2001. Comparison of soil water retention at field and laboratory scales. *Soil Sci. Soc. Am. J.* 65, 460-462.
- Rawls, W.J., Pachepsky, Y., Shen, M.H., 2001. Testing soil water retention estimation with the MUUF pedotransfer model using data from the southern United States. *J. Hydrol.* 251(3), 177-185. [https://doi.org/10.1016/S0022-1694\(01\)00467-X](https://doi.org/10.1016/S0022-1694(01)00467-X)
- Satyanaga, A., Bairakhmetov, N., Kim, J.R., Moon, S.-W., 2022. Role of bimodal water retention curve on the unsaturated shear strength. *Applied Sciences* 12, 1266. <https://doi.org/10.3390/app12031266>
- Szymkiewicz, A., Lewandowska, J., Angulo-Jaramillo, R., Butlańska, J., 2008. Two-scale modeling of unsaturated water flow in a double porosity medium under axisymmetric conditions. *Canadian Geotechnical J.* 45(2), 238-251. <https://doi.org/10.1139/T07-096>
- Świtoniak, M., Kabała, C., Charzyński, P., Capra, G.F., Czigiány, S., Pulido-Fernández, M., *et al.*, 2022. Illustrated Handbook of WRB Soil Classification. Wrocław, Poland. Publisher: Wydawnictwo Uniwersytetu Przyrodniczego, Wrocław, Poland.
- Tian, Z., Gao, W., Kool, D., Ren, T., Horton, R., Heitman, J.L., 2018. Approaches for estimating soil water retention curves at various bulk densities with the extended van Genuchten model. *Water Res. Res.* 54, 5584-5601. <https://doi.org/10.1029/2018WR022871>
- Tian, Z., Ren, T., Horton, R., Heitman, J.L., 2020. Estimating soil bulk density with combined commercial soil water content and thermal property sensors. *Soil Till. Res.* 196, 104445. [doi:10.1016/j.still.2019.104445](https://doi.org/10.1016/j.still.2019.104445)
- Usovich, B., 2011. Development of physical and statistical parameters of selected soil units, taking into account mathematical modeling (in Polish). Project report "Criteria for assessing the physical condition of selected systematic units of arable soils", Ministry of Science and Higher Education No. N N310 3088 34, 2008-2011, Lublin, 2011, pp. 1-30.
- Usovich B., Lipiec J., 2022. Spatial variability of thermal properties in relation to the application of selected soil-improving cropping systems (SICS) on sandy soil. *Int. Agrophys.* 36(4), 269-284. <https://doi.org/10.31545/intagr/152122>
- Usovich, B., Paluszek, J., Rejman, J., 2011. Modeling of water retention curve of variously textured Orthic Luvisols. 28. 28th Congress of Polish Society of Soil Science, Toruń, 5-10.09.2011. Program and abstracts p.145.
- van Genuchten, M.T., 1980. A closed-form equation for predicting the hydraulic conductivity of unsaturated soils. *Soil Sci. Soc. Am. J.* 4, 892-898.
- van Genuchten, M.T., Pachepsky, Y.A., 2011. Hydraulic properties of unsaturated soils. In: J. Gliński, J. Horabik, J. Lipiec (Eds) *Encyclopedia of Agrophysics*, Springer Dordrecht, Heidelberg, London, New York, 368-376.
- van Looy, K., Bouma, J., Herbst, M., Koestel, J., Minasny, B., Mishra, U., *et al.*, 2017. Pedotransfer functions in Earth system science: Challenges and perspectives. *Rev. Geophys.* 55, 1199-1256. <https://doi.org/10.1002/2017RG000581>
- Vizitiu O., Calciu I., Pănoiu I., Simota C., 2011. Soil physical quality as quantified by S index and hydrophysical indices of some soils from Arges hydrographic basin. *Res. J. Agric. Sci.* 43, 249-261.
- Vogel, H.-J., 2019. Scale issues in soil hydrology. *Vadose Zone J.* 18: 190001. <https://doi.org/10.2136/vzj2019.01.0001>
- Wang, M., Wang, J., Xu, G., Zheng, Y., Kang, X., 2021. Improved model for predicting the hydraulic conductivity of soils based on the Kozeny-Carman equation. *Hydrol. Res.* 52, 719-733. <https://doi.org/10.2166/nh.2021.268>
- Wang, Y., Ma, R., Zhu, G., 2022. Improved prediction of hydraulic conductivity with a soil water retention curve that accounts for both capillary and adsorption forces. *Water Res. Res.* 58, e2021WR031297. <https://doi.org/10.1029/2021WR031297>
- Wösten, J.H.M., Lilly, A., Nemes, A., Le Bas, C., 1999. Development and use of a database of hydraulic properties of European soils. *Geoderma* 90, 169-185. [https://doi.org/10.1016/S0016-7061\(98\)00132-3](https://doi.org/10.1016/S0016-7061(98)00132-3)